Accepted Manuscript

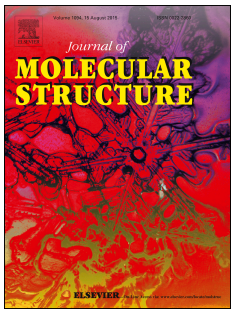

Synthesis, spectroscopic characterization, DFT optimization and biological activities of Schiff bases and their metal (II) complexes

Abdur Rauf, Afzal Shah, Khurram Shahzad Munawar, Abdul Aziz Khan, Rashda Abbasi, Muhammad Arfat Yameen, Asad Muhammad Khan, Abdur Rahman Khan, Irfan Zia Qureshi, Heinz-Bernhard Kraatz, Zia-ur-Rehman

PII: S0022-2860(17)30709-3

DOI: 10.1016/j.molstruc.2017.05.098

Reference: MOLSTR 23839

To appear in: *Journal of Molecular Structure*

Received Date: 22 March 2017

Revised Date: 18 May 2017

Accepted Date: 21 May 2017

Please cite this article as: A. Rauf, A. Shah, K.S. Munawar, A.A. Khan, R. Abbasi, M.A. Yameen, A.M. Khan, A.R. Khan, I.Z. Qureshi, H.-B. Kraatz, Zia-ur-Rehman, Synthesis, spectroscopic characterization, DFT optimization and biological activities of Schiff bases and their metal (II) complexes, *Journal of Molecular Structure* (2017), doi: 10.1016/j.molstruc.2017.05.098.

Synthesis, spectroscopic characterization, DFT optimization and biological activities of Schiff bases and their metal (II) complexes

Abdur Rauf[a,*], Afzal Shah[b,*], Khurram Shahzad Munawar[c], Abdul Aziz Khan[d], Rashda Abbasi[e], Muhammad Arfat Yameen[f], Asad Muhammad Khan[a], Abdur Rahman Khan[a], Irfan Zia Qureshi[d], Heinz-Bernhard Kraatz[g], Zia-ur-Rehman[b]

a. Department of Chemistry, COMSATS Institute of Information Technology, Abbottabad 22060, Pakistan
b. Department of Chemistry, Quaid-i-Azam University, 45320 Islamabad, Pakistan
c. Department of Chemistry, School of Science, University of Management and Technology, Lahore, Pakistan
d. Department of Animal Sciences, Quaid-i-Azam University, 45320 Islamabad, Pakistan
e. Institute of Biomedical and Genetic Engineering Islamabad, Pakistan
f. Department of Pharmacy, COMSATS Institute of Information Technology, Abbottabad 22060, Pakistan
g. Department of Physical and Environmental Sciences, University of Toronto, 1265 Military Trail, Toronto M1C 1A4, Canada

*To whom correspondence should be addressed

E-mails: raufrazi41@41hotmail.com (A. Rauf), afzals_qau@yahoo.com (A. Shah)

Graphical Abstract

Two Schiff bases and their Zinc (II) and cobalt (II) complexes were synthesized and confirmed. Their DFT optimizations, pH dependent photometry and biological activities were evaluated in detail. Some of the compounds being good antidiabetic, antibacterial and cytotoxic agents were found astonishing candidate for drug development.

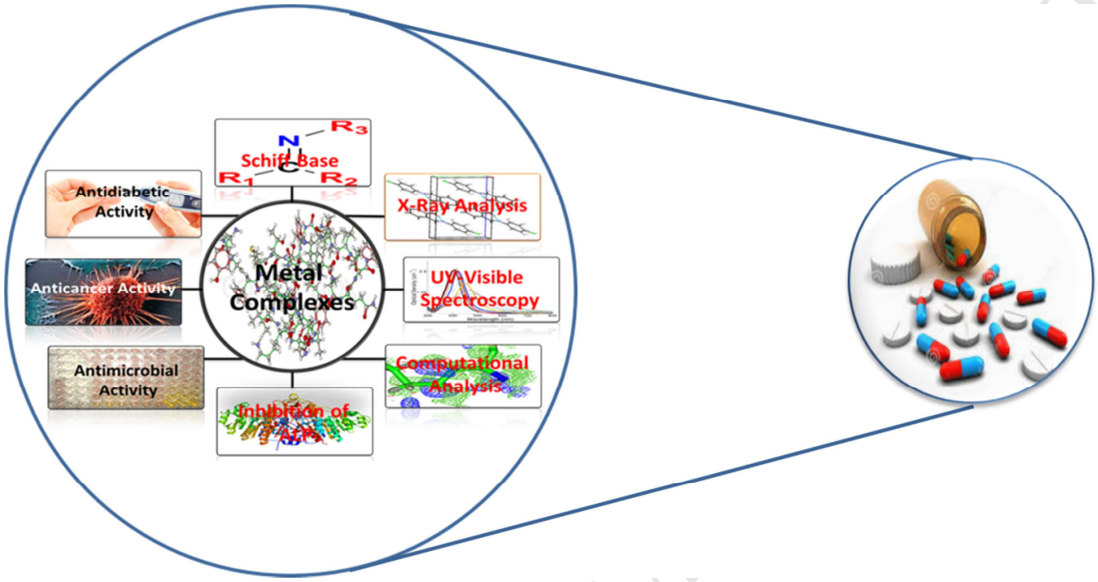

Abstract

A Novel Schiff base, 3-(((4-chlorophenyl)imino)methyl)benzene-1,2-diol (***HL*^{1}**) was successfully synthesized along with a structurally similar Schiff base 3-(((4-bromophenyl)imino)methyl)benzene-1,2-diol (***HL*^{2}**). Both the Schiff bases were used to synthesize their zinc (II) and cobalt (II) complexes. These compounds were characterized by FTIR, ^{1}H NMR, ^{13}C NMR and elemental analysis. Metal complexes were confirmed by TGA. Crystals of Schiff bases were also characterized by X-ray analysis and experimental parameters were found in line with the theoretical parameters. Quantum mechanical approach was also used to fine useful structural parameters and to ensure the geometry of metal complexes. The photometric behaviors of all the synthesized compounds were investigated in a wide pH range using BR buffers. The appearance of isosbestic points indicated the existence of Schiff bases in more than one isomeric form. Moreover, these compounds were screened for enzyme inhibition; antibacterial, cytotoxic and *in vivo* antidiabetic activities and compounds were found active against one or other activity. Results indicate that $\boldsymbol{ZnL_2^2}$ is a good inhibitor of alkaline phosphatase enzyme and possess highest potential against diabetes, blood cholesterol level and cancer cells. This effort just provides preliminary data for some

biological properties. Further investigations are required to precisely determine mechanistic pathways of their use towards drug development.

Keywords: Schiff Base; Metal-Schiff base complexes; Spectroscopy; X-ray analysis; antibacterial activity, antidiabetic activity, cytotoxicity

1. Introduction

Schiff bases are the organic compounds containing azomethine/ imine (–C=N–) functional group. They were first reported by Hugo Schiff and can be synthesized by the condensation reaction of amines with carbonyl compounds [1, 2]. Plethora of Schiff base derivatives is also present in natural and natural-derived compounds like ancistrocladidine and chitosan derived Schiff bases [3]. Numerous Schiff bases have been reported to exhibit remarkable biological activities containing antibacterial, antifungal, antimalarial, anti-proliferative, anti-inflammatory, antiviral, and antipyretic properties [4] and the imine group present in such compounds is thought to be responsible for such properties [5-7]. Cleiton *et al*. have explored antibacterial activities of several compounds [3]. Pandeya *et al*. reported strong antibacterial activities of 5-chloro-salicylaldehyde derived and Isatin-derived Schiff bases [8]. N-(salicylidene)-2-hydroxyaniline has been reported to show inhibitory action against Mycobacterium tuberculosis H37Rv [6]. Similarly, 2,4-dichloro-5-fluorophenyl derivatives was reported to inhibit the growth of *E. coli*, *S. aureus, Klebsiella pneumoniae, Aspergillus fumigatus, Aspergillus flavus, Trichophyton mentagrophytes, Penicillium marneffei* and *Pseudomonas aeruginosa* [9]. Very small amount of N-(Salicylidene)-2-hydroxyaniline was reported to significantly inhibit the growth of fungi [10]. Literature survey reveals that chitosan derived Schiff bases were efficiently used as inhabitant against the growth of *Botrytis cinerea* and *Colletotrichum lagenarium* [7]. 1-amino-3-hydroxyguanidine tosylate-derived Schiff bases were indicated to be very effective against mouse hepatitis virus (MHV), inhibiting its growth [11]. Vitamin B6, a Schiff base derivative of pyridoxine is reported to abolish the enzyme activities of proteins [12]. Beside inhibitory action, catalytic properties of Schiff bases have been reported like plant hormone and plant growth regulatory activity towards cytokine and auxin [13-15]. Their photometric and thermochemical properties make them useful in modern applications including solar filters, photodetectors, photostabilizers, microelectronic devices and optical switches [16-20].

Due to the presence of lone pair on sp^2 hybridized N atom, Schiff bases are able to produce metal complexes, polycyclic quinoline derivatives and numerous heterocyclic compounds [16, 21-25]. Their reactivity increases exponentially in the presence of –OH groups especially when the –OH group is present at –ortho position [26-31]. Research in this field has received utmost attention because induction of metals to Schiff base structures robust their properties manifold and makes them more applicable. They are good catalysts and catalyst producing agents because of their greater redox activities [32-34]. Due to their

structural diversity they are used in stereo chemistry [35, 36] and medicinal applications [37]. They are used to produce dyes and pigments [3]. DNA interacting modes of these metal complexes make them useful as new therapeutic agents [38]. Transition metal complexes of bipyridine and phenanthroline are used in petroleum industry [39]. Hamada and Kawamoto reported the use of metal complexes as an effective emitting layer and luminescent compounds [40-42]. Schiff bases and their metal complexes have been well explored and reviewed. Although a number of reviews are available to disclose the effect of metal on the properties of Schiff bases. Silva *et al*. proposed that Schiff bases derived from salicylaldehyde may provide a platform to produce useful compounds with desirable biological and industrial properties [11, 43], therefore in this research work, salicylaldehyde derivative is used to synthesize Schiff bases and metallic complex. An effort is made to explore its physicochemical properties.

2. Experimental

2.1 Materials and Reagents

2,3-Dihydroxybenzaldehyde, 4-chloroaniline and 4-bromoaniline were received from Sigma Aldrich, USA. Zinc acetate and cobalt acetate were obtained from Fluka, Switzerland. The analytical grade solvents like, chloroform, n-hexane, ethanol and dimethyl sulfoxide were obtained from Merck, Germany. All BRB solutions were prepared according to reported protocol [44, 45] using analytical-grade reagents and doubly distilled water with (conductivity $\leq$0.1 μScm^{-1}). All experiments were carried out at room temperature (25±1 ºC).

2.2 Instrumentation and measurement

Thermo Nicolet 6700 FTIR spectrophotometer was used to obtain IR spectra in the range of 4000–100 cm^{-1}. ^{1}H and ^{13}C NMR were recorded on Bruker AC Spectrometers with tetramethylsilane (TMS) as internal reference. Absorption spectra were recorded on Shimadzu 1601 spectrophotometer and the pH measurements were carried out with a Crison micro pH 2001 pH-meter with an Ingold combined glass electrode. GAUSSIAN 09 software was used to find geometry of Schiff bases and their metal complexes using 6-31++G** and 6-31G^{++} basis sets, respectively. Summary of the different calculated parameters is given in Table 6.

2.3 Synthesis of Schiff base ligands

3-(((4-chlorophenyl)imino)methyl)benzene-1,2-diol (HL^1)

Schiff bases were prepared by mixing equimolar amounts of 2,3-dihydroxybenzaldehyde and respective 4-haloaniline in freshly dried ethanol. After refluxing for 2 hours, red crystalline solid product was appeared which was cooled, filtered and further processed for crystallization in a mixture of chloroform and n-hexane (3:1).

$C_{13}H_{10}ClNO_2$: Mol. Wt. 247.68 gmol^{-1}, Yield 87 %, M.P. 127.5 ^{o}C; FT-IR (KBr, υ/cm^{-1}): 3445 (OH phenolic), 3032 (CH Aromatic), 1617 (HC=N Schiff base), 1463 (C=C Aromatic), Anal. Calc.: C, 62.73; H, 4.06; N, 5.63. Found: C, 61.52; H, 3.91; N, 5.49 %. ^{1}H NMR (DMSO-d_6, ppm, 400 MHz) δ: 8.58 (s, 1H, CH=N), 12.52 (s, 1H, OH), 9.32 (s, 1H, OH), 6.84 (t, 1H), 7.05 (dd, 1H), 6.95 (dd, 1H), 7.52 (d, 2H), 7.02 (d, 2H), ^{13}C NMR (DMSO-d_6, ppm, 101 MHz) δ: 163.42 (CH=N), 149.5 (C-OH), 149.1 (C-OH), 145.3 (C-N), 119.6-132.8 (Aromatic Carbons).

3-((4-bromophenyl)imino)methyl)benzene-1,2-diol (HL^2)

$C_{13}H_{10}BrNO_2$: Mol. Wt. 292.13 gmol^{-1}, Yield 83 %, M.P. 150.2 ^{o}C; FT-IR (KBr, υ/cm^{-1}): 1620 (HC=N Schiff base), 3448 (OH phenolic), 3080 (CH Aromatic), 1462 (C=C Aromatic), Anal. Calc.: C, 53.40; H, 3.46; N, 4.79. Found: C, 53.28; H, 3.30; N, 4.65 %. ^{1}H NMR (DMSO-d_6, ppm, 400 MHz) δ: 8.56 (s, 1H, CH=N), 11.08 (s, 1H, OH), 9.87 (s, 1H, OH), 6.83 (t, 1H), 7.07 (dd, 1H), 6.92 (dd, 1H), 7.75 (d, 2H), 7.15 (d, 2H), ^{13}C NMR (DMSO-d_6, ppm, 101 MHz) δ: 162.52 (CH=N), 149.4 (C-OH), 149.0 (C-OH), 150.3 (C-N), 119.6-132.9 (Aromatic Carbons).

2.4 Synthesis of transition metal (II) complexes

All the metal complexes were prepared by the following method. Corresponding metal (II) acetate salt was added to hot ethanol solution of Schiff base ligand in molar ratio 2:1 respectively. In few minutes, the colored complex was precipitated out in each case. The complexes were filtered and washed with ethanol.

bis(2-(((4-chlorophenyl)imino)methyl)-6-hydroxyphenoxy)zinc (ZnL_2^1)

$C_{26}H_{18}Cl_2N_2O_4Zn$: Mol. Wt.: 558.72 gmol^{-1} Yield: 74 %, M.P. 278.3 ^{o}C; FT-IR (KBr, υ /cm^{-1}): 1574 (HC=N Schiff base), 3060 (CH Aromatic), 1443 (C=C Aromatic), 450 (Zn-O), 428 (Zn-N); Anal. Calc.: C, 56.12; H, 3.27; N, 5.04. Found: C, 55.97; H, 3.01; N, 4.88 %. ^{1}H NMR (DMSO-d_6, ppm, 400 MHz) δ: 8.43 (s, 1H, CH=N), 9.82 (s, 1H, OH), 6.82 (t, 1H), 7.06 (dd, 1H), 6.91 (dd, 1H), 7.51 (d, 2H), 7.78 (d, 2H), ^{13}C NMR (DMSO-d_6, ppm, 101

MHz) δ: 158.7 (CH=N), 145.4 (C-O), 147.24 (C-OH), 151.7 (C-N), 119.6-132.8 (Aromatic Carbons).

bis(2-(((4-bromophenyl)imino)methyl)-6-hydroxyphenoxy)zinc (ZnL_2^2)

$C_{26}H_{18}Br_2N_2O_4Zn$: Mol. Wt.: 647.62 gmol^{-1} Yield: 78 %, M.P. 243.6 ^oC; FT-IR (KBr, υ /cm^{-1}): 1576 (HC=N Schiff base), 3018 (CH Aromatic), 1446 (C=C Aromatic), 443 (Zn-O), 418 (Zn-N). Anal. Calc.: C, 48.18; H, 2.81; N, 4.32. Found: C, 48.02; H, 2.63; N, 4.09 %. ^{1}H NMR (DMSO-d_6, ppm, 400 MHz) δ: 8.39 (s, 1H, CH=N), 9.78 (s, 1H, OH), 6.81 (t, 1H), 7.20 (dd, 1H), 6.86 (dd, 1H), 7.20 (d, 2H), 7.75 (d, 2H), ^{13}C NMR (DMSO-d_6, ppm, 101 MHz) δ: 158.5 (CH=N), 145.5 (C-O), 147.38 (C-OH), 152.8 (C-N), 119.6-132.9 (Aromatic Carbons).

bis(2-(((4-chlorophenyl)imino)methyl)-6-hydroxyphenoxy)cobalt (CoL_2^1)

$C_{26}H_{18}Cl_2N_2O_4Co$: Mol. Wt.: 552.27 gmol^{-1} Yield: 79 %, M.P. > 300 ^oC; FT-IR (KBr, υ /cm^{-1}): 1578 (HC=N Schiff base), 3019 (CH Aromatic), 1441 (C=C Aromatic), 541 (Co-O), 466 (Co-N); Anal. Calc.: C, 56.49; H, 3.29; N, 5.07. Found: C, 56.25; H, 3.06; N, 4.89 %.

bis(2-(((4-bromophenyl)imino)methyl)-6-hydroxyphenoxy)cobalt (CoL_2^2)

$C_{26}H_{18}Br_2N_2O_4Co$: Mol. Wt.: 641.17 gmol^{-1} Yield: 82 %, M.P. 291.5 ^oC; FT-IR (KBr, υ /cm^{-1}): 1572 (HC=N Schiff base), 3022 (CH Aromatic), 1452 (C=C Aromatic), 538 (Co-O), 458 (Co-N). Anal. Calc.: C, 48.66; H, 2.84; N, 4.37. Found: C, 48.55; H, 2.60; N, 4.15 %.

TGA data of metal complexes is given in Table 1.

2.5 X-Ray Structure Determination

Single crystals of ***HL^1*** and ***HL^2*** were used to investigate structural arrangements using Microstar diffractometer at 100 K. Charge Flipping program was used to solve the structure with olex2 [46] and refined with XL [47] refinement package using least squares minimization. Data and details of crystal structure are given in Tables 2-4.

2.6 Assay of alkaline phosphatase activity

Synthesized Schiff bases and their metal complexes were investigated for inhibition of alkaline phosphatase (ALP) enzyme as the reported procedure [47]. *p*-Nitrophenyl phosphate was hydrolyzed in the presence of ALP, Mg^{2+} ions and phosphate buffer of pH 9.8 to produce yellow colored *p*-nitrophenol (Scheme 1) and the progress was monitored by measuring its

absorbance values at 405 nm. Finally different amounts of the synthesized compounds were added periodically from stock DMSO solution and absorbance was measured again after incubation. Each experiment was repeated thrice and average values were used to calculate percentage inhibition.

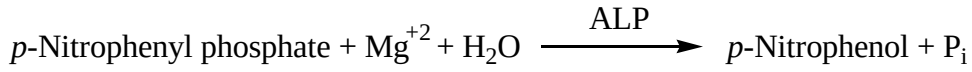

Scheme 1. Hydrolysis of alkaline phosphatase
where P_i is inorganic phosphate.

2.7 Quantitative antibacterial activity assay by minimum inhibitory concentration

In vitro Serial dilution microplate method was used for determination of MIC on *Staphylococcus aureus* and *Escherichia coli* bacteria according to previously described methods with some modifications [48, 49]. The test samples were dissolved in DMSO/Mueller Hinton Broth (MHB). The final concentration of DMSO was kept lower than 2.5% so it may not affect the bacterial growth. The prepared test samples (100µl) were added to the first well of a 96-well microtiter plate and serially diluted two fold. Overnight grown bacterial cultures were adjusted to 0.5 McFarland standards and 100µl were added to each well. The plates were incubated at 37°C for 18 hrs. The assay was performed in triplicate. Wells containing MHB with 100µl of inoculum and DMSO to a final concentration of 2.5% served as negative control. The MIC of samples was measured by the addition of 40 µl of 1 mg/5 mL of p-iodonitrotetrazolium violet (INT) and incubated at 37°C for 30 min. The lowest sample concentration that prevent the color change of the medium by the addition of INT, demonstrated the complete inhibition of microbial growth [48]. Microplates with experimental results can be seen in Fig. S1-S4 and MIC values are given in Table 7.

2.8 *In vitro* anti-cancer activity

2.8.1 Cell culture

Human hepatocellular carcinoma HepG2 (ATCC HB-8065™) cell line was cultured in DMEM supplemented with FBS (10%), Na-pyruvate (1 mM), L-glutamine (2 mM), penicillin (100 U/ml) and streptomycin (100 µg/ml). The cultures were maintained at 37°C and 5% CO_2 under humidified conditions.

2.8.2 Cytotoxicity analysis

In vitro cytotoxicity analysis of the compounds was done by sulforhodamine B (SRB) assay as described earlier [50]. In short, actively growing HepG2 cells (10000 cells/well) were exposed to the compounds at 200 μM concentration for 24 hrs under standard culture conditions. Untreated and DMSO (solvent) treated cultures were included as experimental control. Cultures were fixed using pre-chilled trichloroacetic acid (50%) for 1 h at 4°C, washed thoroghly with deionized water and air dried. The cells were then stained with SRB solution (0.05%) for 30 minutes, washed with acetic acid (1%), dried overnight and photographed with a Olympus IMT-2 inverted microscope equipped with digital camera. The incorporated dye was solubilized in 10 mM Tris and absorbance (OD) was measured on microplate reader (AMP PLATOS R-496) at the wavelength of 565 nm. Percent (%) viability was calculated relative to the untreated sample using the following formula

Percent (%) viability = $[Abs(565)_{test\ sample}-Abs(565)_{compound\ control} / Abs(565)_{untreated\ sample}-Abs(565)_{blank}] \times 100$

Where, $Abs(565)_{test\ sample}$ and $Abs(565)_{untreated\ sample}$ is OD for cultures treated and untreated samples, respectively. $Abs\ (565)_{compound\ control}$ and $Abs\ (565)_{blank}$ is the OD measured in compounds only and media only samples.

2.8.3 Statistical analysis

The results presented as mean ± SD were analyses by ANOVA and two tailed t-test. Differences between untreated and treated samples were investigated. Further, metal complexes were compared with their respective Schiff bases. Results were considered significant when $p<0.05$.

2.9 *In vivo* Antidiabetic Activity

2.9.1 Animals Maintenance and Treatment

A total of fifty healthy adult male Sprague–Dawley rats (average body wt = 255 ± 19g) obtained from the National Institute of Health Islamabad and were maintained at the Animal House Facility of the Animal Sciences Department, Quaid-i-Azam University Islamabad. Five rats were housed per single cage and had free access to standard rodent diet and drinking water maintained, while photoperiod conditions were 12hL:12hD. A total of eight groups (n = 5) were made diabetic through a single dose (150 mg/kg b.w) of alloxan monohydrate (Sigma Aldrich, USA) administered intraperitonaly to overnight fasted rats. Six groups were treated with six different compounds; $\boldsymbol{HL^1}$, $\boldsymbol{HL^2}$, $\boldsymbol{ZnL_2^1}$, $\boldsymbol{ZnL_2^2}$, $\boldsymbol{CoL_2^1}$ and $\boldsymbol{CoL_2^2}$ with acute dose of 35.0 mg/kg b.w while the control groups, positive and negative were treated with

antidaibetic compound glibenclamide (10mg/kg b.w) dissolved in distilled H_2O, (Euglucon, Roche Pharma) and normal saline respectively [51].

2.9.2 Glucose, Triglycerides and Cholesterol Determination

Glucose level was determined from blood samples collected from the caudal vein at different times. Two samples were drawn before treatments with compounds (dissolved in DMSO) (-1 pre alloxan sample and 0 post alloxan sample) and seven samples were drawn at one hour interval (1, 2, 3, 4, 5, 6 and 7hr) post treatment with compounds. The plasma level of glucose was determined with a glucometer (Accu-Check Active,Roche) and dextrostix strips. Triglycerides and cholesterol level were determined through commercially available kits obtained from the Globe Diagnostic (Italy), following the standard procedure given in along with each kit.

2.9.3 Statistical Analysis

Data were analyzed through one-way analysis of variance (ANOVA) to compare the means between groups, followed by Post hoc Bonferroni tests for multiple comparisons among different groups. Data are presented by line or bar graphs as mean ± S.D, while $P < 0.05$ was considered statistically significant difference.

3. Results and Discussion

3.1 Structural Characterization

FTIR spectra of ***HL*^{1}** and ***HL*^{2}** showed a strong absorption band in the range 1617-1620 cm^{-1} due to azomethine group indicating the formation of Schiff bases. Moreover, appearance of resonance signals related to azomethine proton and carbon in ^{1}H and ^{13}C NMR spectra respectively confirmed the formation of Schiff bases. Absence of primary amine peak revealed their purity. Zn metal complexes were confirmed by the shifting of azomethine signal to longer wavelength (1574-1576 cm^{-1}) in FTIR spectra and by downfield shifting of azomethine resonance signals in the NMR spectra. Disappearance of proton resonance signal related to ortho-hydroxyl group also ensured the coordination of ligand molecules with zinc ions. Thermogravimetric analysis of metal complexes was carried out from ambient temperature to 1000 °C in nitrogen atmosphere. The summary of decomposed fragments against various temperature ranges is summarized in the Table 1. These observations are in line with elemental analyses. No weight loss around $100^{o}C$ ensured absence of water

molecules in coordinated structures. In all cases fragmentation took place in one step with the loss of ligands and metal oxides left in the form of residue.

3.2 Crystal structures description

Crystal structure of $\boldsymbol{HL^1}$ is depicted in Fig. 1 along with crystal packing and numbering scheme. Summary of structural refinements and crystal data can be seen in Table 2. Selected bond distances and bond angles for $\boldsymbol{HL^1}$ are presented in Table 3 and compared with DFT calculated parameters. Critical review of the data reveals that the novel Schiff base $\boldsymbol{HL^1}$ belongs to triclinic crystal system and have non-planar geometry as reported for $\boldsymbol{HL^2}$ [52]. Smaller N-C7 bond length as compared to N-C8 ensures double bond character in the N-C7 bond and existence of molecule in enolic form as supported by computational results. Distorted hexagonal rings can be justified by the presence of attached groups. There is a possibility of intermolecular as well as intramolecular hydrogen bonding as shown in Table 4 and Fig. 1. Experimental parameters were found in good agreement with the calculated values. In case of $\boldsymbol{HL^2}$, results were found similar as reported by Shuja *et al*. [52].

3.3 Electronic absorption spectroscopy

Fig. 2 depicts absorption spectra of 13.8 µM solutions of ligands and their metal complexes in 9:1 mixture of ethanol and DMSO. $\boldsymbol{HL^1}$ exhibits an intense band at 222 nm and a less intense doublet with maxima at 250 and 266 nm. The intense band is thought to be due to π–π* transitions of aromatic rings while less intense doublet can be assigned to π–π* transitions of –C=N group and –C=O group which arises due to tautomerism [47]. In case of $\boldsymbol{HL^2}$ these bands shifted to 225, 284 and 318 nm, respectively. This red shift can be attributed to the increase in electron density due to less electronegative nature of –Br group hence decreasing the required energies for transitions [47]. Further observation of Fig. 2 reveals that all the metal complexes have different photometric behavior as compared to ligands due to change in their orbital energies and band gap values shown by the computational results (Table 6). Moreover, appearance of new peaks in the range of 215-235 nm and 370-500 nm offers the strong evidence of complexation. Shifting of signals related to azomethine and carbonyl groups towards larger wavelength suggests a significant charge transfer from metal orbitals to ligand orbitals (LMCT) [51]. Appearance of (less intense) new peaks after 450 nm can be assigned to d-d transitions which were used to find the geometry of the complexes by calculating their extinction coefficients. 554 and 811 m^2 mol^{-1} ε values suggest $\boldsymbol{ZnL_2^2}$ and $\boldsymbol{CoL_2^2}$ to have tetrahedral geometries [53, 54]. Geometries of $\boldsymbol{ZnL_2^1}$ and $\boldsymbol{CoL_2^1}$ can't be predicted due to absence of charge transfer band.

The absorption spectra of 20 μM ***HL*^{1}** and ***HL*^{2}** in different pH media are shown in Fig.3. Observation of the spectra reveals that pH of the medium strongly affects the photometric behavior of both the ligands. Increase in the alkalinity of the medium results in bathochromic shift. This shift can be explained by the removal of proton from –OH group leaving negative charge on oxygen atom which makes the transition more feasible [55]. Appearance of isosbestic points in the range of 253-351 nm indicates the existence of equilibrium between different mesomeric forms of the molecules. In case of metal complexes no significant change was observed with increase in pH probably due to M-O bonds. λ_{max}, ε and pK_a values for ligands and their complexes are summarized in Table 5.

3.4 Computational Studies

Structures of Schiff bases and their metal complexes were optimized using 6-31++G** and 6-31G^{++} basis sets, respectively due to complexity of metal complexes. Results reveal that both the ligands possess non planar structures as reported for such molecules [47]. Bond lengths obtained from DFT studies were compared with experimental results obtained from X-ray analysis and found in good agreement (Table 3). Metal complexes were found to possess tetrahedral geometries as shown in Fig. 4. The most stable confirmation was also used to calculate different useful parameters like total energy, dipole moment, E_{HOMO}, E_{LUMO}, band gap energy ($\Delta E = E_{HOMO} - E_{LUMO}$), ionization energy, electron affinity, Electronegativity (Table 6). These calculations ensure about the geometries of metal complexes and offer better explanation to the experimental findings.

3.5 Inhibition of ALP

Alkaline phosphatases (ALPs) are dimeric metallic enzymes having zinc metal ions in each active site [47] . In bacteria they are present in periplasmic space while in humans they are present in all body tissues but mainly in kidney, placenta and intestinal mucosa [56]. They are one of the clinical important enzymes as they act as catalysts in dephosphorylation and their abnormal amount causes several diseases including anemia, hypophosphatasia, hypothyroidism, osteoporosis, leukemia, lymphoma, breast cancer and sarcoidosis [57, 58]. Metal complexes of Schiff bases are found to be best inhibitors of phosphatase enzymes [59] as they can block their active cites, therefore synthesized compounds were screened for inhibitory action. All the compounds were found to reduce the activity of enzyme in concentration dependent manner (Fig. 5); however presence of metal ions enhanced this

inhibitory action as expected. $\boldsymbol{ZnL_2^2}$ has shown best results with 80% inhibition at 500 µM concentration.

3.6 Antibacterial activity

Compounds $\boldsymbol{HL^1}$, $\boldsymbol{ZnL_2^1}$ and $\boldsymbol{HL^2}$ have shown moderate antibacterial activity (<100µg/ml) against *E. coli* while $\boldsymbol{HL^1}$ and $\boldsymbol{CoL_2^1}$ have moderate antibacterial activity against *S. aureus*. Rest of all the compounds have low antibacterial activity (>100µg/ml) against both the bacteria [60]. Microplates with experimental results can be seen in Fig. S1-S4 and MIC values are summarized in Table 7.

3.7 *In vitro* Cytotoxicity analysis

The Schiff bases and their metal complexes were investigated for cytotoxic potential against HepG2 cell line (Fig. 6 & 7). Cultures were exposed to the compounds (200 µg/ml) for 24 hours, and then analyzed by SRB assay. Data showed that both $\boldsymbol{ZnL_2^2}$ (relative viability = 26.67 ± 3.97) and $\boldsymbol{CoL_2^2}$ (relative viability = 32.53 ± 2.54) were biologically active against HepG2 cells, whereas $\boldsymbol{HL^2}$ exhibited slight toxicity against the cultures. On the other hand $\boldsymbol{HL^1}$ (relative viability = 36.78 ± 2.85) was more toxic when compared to $\boldsymbol{ZnL_2^1}$ and $\boldsymbol{CoL_2^1}$. Furthermore, $\boldsymbol{ZnL_2^2}$ and $\boldsymbol{CoL_2^2}$ also induced morphological changes in the cells causing cellular clumping and blebbing thus leading to apoptosis [61, 62].

3.8 *In vivo* Antidiabetic Activity

Compound $\boldsymbol{HL^1}$ showed high level of diabetic activity. The rats treated with compound $\boldsymbol{HL^1}$ had higher blood glucose level as compared to positive control group ($P < 0.001$), while no significant difference was observed in comparison with compounds $\boldsymbol{ZnL_2^1}$, $\boldsymbol{CoL_2^1}$ and the negative control group. Compound $\boldsymbol{ZnL_2^1}$ and $\boldsymbol{CoL_2^1}$ aslo drastically increased glucose level as compared to positive control group ($P < 0.001$), (Fig. 8A).

In contrast compound $\boldsymbol{ZnL_2^2}$ had better antidiabetic potential than $\boldsymbol{HL^2}$and $\boldsymbol{CoL_2^2}$ compounds. The blood glucose level of the rats treated with compound $\boldsymbol{ZnL_2^2}$ was lower as compared to $\boldsymbol{HL^2}$ treated group, $\boldsymbol{CoL_2^2}$ treated group and negative control group ($P < 0.001$ in all cases). The antidiabetic potential of $\boldsymbol{ZnL_2^2}$ was almost similar to the reference antidiabetic compound (Fig. 8B).

A high level of similarity was found in the level of diabetic potential between $\boldsymbol{HL^1}$ and $\boldsymbol{ZnL_2^1}$ compounds and between $\boldsymbol{CoL_2^1}$ and $\boldsymbol{CoL_2^2}$ compounds. The blood glucose level of the treated

rats with these four compounds was significantly higher than the positive control group ($P < 0.001$), while comparable with the negative control group ($P > 0.5$; Fig. 8 A&B).

Compound $\boldsymbol{HL^1}$ treatment significantly increased the serum triglycerides concentration compared to HL^2 treatment ($P < 0.01$) and both negative and positive control groups ($P < 0.001$) but the concentration was found decreased as compared to $\boldsymbol{CoL_2^1}$ treated animals ($P < 0.001$). Likewise, compound $\boldsymbol{HL^2}$ led to significant increase concentration of triglycerides as compared to $\boldsymbol{ZnL_2^2}$, $\boldsymbol{CoL_2^2}$ ($P < 0.001$), and positive control group ($P < 0.01$). In contrast the concentration of serum triglycerides was drastically decreased with $\boldsymbol{ZnL_2^2}$ treatment in comparison with $\boldsymbol{ZnL_2^1}$ treated animals and negative control group ($P < 0.001$), while treatment with compound $\boldsymbol{CoL_2^2}$ caused a decrease in serum triglycerides concentration in comparison with $\boldsymbol{CoL_2^1}$, negative ($P < 0.001$) and positive control groups ($P < 0.5$), (Fig. 8C). A highly significant decrease was observed in the cholesterol level of the animals treated with compounds $\boldsymbol{HL^1}$ ($P < 0.01$), $\boldsymbol{ZnL_2^1}$ ($P < 0.05$), $\boldsymbol{CoL_2^1}$ ($P < 0.05$), $\boldsymbol{HL^2}$ ($P < 0.001$), and $\boldsymbol{CoL_2^2}$ ($P < 0.01$) in comparison with the negative control group animals. The concentration of cholesterol did not decrease with $\boldsymbol{ZnL_2^2}$ treatment in comparison with negative control group rats ($P > 0.5$), however highly significant increase as compared to $\boldsymbol{HL^2}$ ($P < 0.01$) and $\boldsymbol{CoL_2^2}$ ($P < 0.5$) compounds (Fig. 8D).

4 Conclusion

Two Schiff bases and their four metal complexes were synthesized and characterized by various techniques. FTIR, NMR, elemental analysis and TGA ensured the formation of compounds. XRD results indicated the existence of H-bonding in Schiff base molecules and DFT results also supported these findings. Computational results were also used to explain ensure the geometry of metal complexes and finding useful energy parameters. Photometric signature of Schiff bases was found to be strongly pH dependent. Furthermore, metal complexes were found good inhibitors of alkaline phosphatase enzyme than Schiff bases. Results of antibacterial, anticancer and antidiabetic activities reveal that some of these compounds have good potential to be used in drug development. $\boldsymbol{ZnL_2^2}$ was found to be most active against cancer cell as well as diabetes. $\boldsymbol{HL^2}$ have shown markable decrease in blood cholesterol level. Further efforts should be made to precisely explore the possible mechanistic pathways of their activity *in vivo* as well as *in vitro*.

Acknowledgements

The authors gratefully acknowledge the financial support of the Higher Education Commission of Pakistan through project number 21-1209, CIIT Abbottabad and Quaid-i-Azam University Islamabad.

Appendix A. Supplementary material

CCDC reference number 210655. See http://www.rsc.org/suppdata/dt/b3/b305443h/ for crystallographic data in CIF or other electronic format.

References:

[1] Cimerman Z, Miljanić S, Galić N. Schiff bases derived from aminopyridines as spectrofluorimetric analytical reagents. Croatica Chemica Acta 2000;73:81-95.

[2] Schiff H. Mittheilungen aus dem Universitätslaboratorium in Pisa: eine neue Reihe organischer Basen. Justus Liebigs Annalen der Chemie 1864;131:118-9.

[3] da Silva CM, da Silva DL, Modolo LV, Alves RB, de Resende MA, Martins CV, et al. Schiff bases: a short review of their antimicrobial activities. Journal of Advanced research 2011;2:1-8.

[4] Przybylski P, Huczynski A, Pyta K, Brzezinski B, Bartl F. Biological properties of Schiff bases and azo derivatives of phenols. Current Organic Chemistry 2009;13:124-48.

[5] Bringmann G, Dreyer M, Faber JH, Dalsgaard PW, Stærk D, Jaroszewski JW, et al. Ancistrotanzanine C and Related 5, 1'-and 7, 3'-Coupled Naphthylisoquinoline Alkaloids from Ancistrocladus t anzaniensis 1. Journal of natural products 2004;67:743-8.

[6] Souza AOd, Galetti F, Silva CL, Bicalho B, Parma MM, Fonseca SF, et al. Antimycobacterial and cytotoxicity activity of synthetic and natural compounds. Química Nova 2007;30:1563-6.

[7] Guo Z, Xing R, Liu S, Zhong Z, Ji X, Wang L, et al. Antifungal properties of Schiff bases of chitosan, N-substituted chitosan and quaternized chitosan. Carbohydrate research 2007;342:1329-32.

[8] Pandeya S, Sriram D, Nath G, De Clercq E. Synthesis and antimicrobial activity of Schiff and Mannich bases of isatin and its derivatives with pyrimidine. Il Farmaco 1999;54:624-8.

[9] Karthikeyan MS, Prasad DJ, Poojary B, Bhat KS, Holla BS, Kumari NS. Synthesis and biological activity of Schiff and Mannich bases bearing 2, 4-dichloro-5-fluorophenyl moiety. Bioorganic & medicinal chemistry 2006;14:7482-9.

[10] Rehman W, Baloch MK, Muhammad B, Badshah A, Khan KM. Characteristic spectral studies andin vitro antifungal activity of some Schiff bases and their organotin (IV) complexes. Chinese Science Bulletin 2004;49:119-22.

[11] Sriram D, Yogeeswari P, Myneedu NS, Saraswat V. Abacavir prodrugs: Microwave-assisted synthesis and their evaluation of anti-HIV activities. Bioorganic & medicinal chemistry letters 2006;16:2127-9.

[12] Tobriya SK. Biological Applications of Schiff base and its Metal Complexes-A Review. Int J Sci Res 2014;3:1254-6.

[13] Huneck S, Schreiber K, Grimmecke HD. Schiffs bases and derived secondary amines as plant growth inhibitors. Journal of plant growth regulation 1984;3:75-84.

[14] Wang Y, Yu X, Lu B, Ye W, Sheng S. plant harmone activity of Schiff base ester of 5-aminotriazole-3-carboxylic acid, Huaxue Shiji, 23 (2001) 257-58, 301. Chem Abstr2002. p. 247530.

[15] Song X, Wang Z, Wang Y, Zhang Z, Chen C. Synthesis and biological activity of Schiff bases of 2-amino-5-(4-pyridyl)-1, 3, 4-thiodiazol, Yingyong Huaxue, 22 (2005) 334-336. Chem Abstr2005. p. 367252.

[16] Tanaka K, Shimoura R, Caira MR. Synthesis, crystal structures and photochromic properties of novel chiral Schiff base macrocycles. Tetrahedron Letters 2010;51:449-52.

[17] Mocanu AS, Iliş M, Dumitraşcu F, Ilie M, Cîrcu V. Synthesis, mesomorphism and luminescence properties of palladium (II) and platinum (II) complexes with dimeric Schiff base liquid crystals. Inorganica Chimica Acta 2010;363:729-36.

[18] Issa YM, Sherif OE, Abbas SM. Chelation behaviour of Ce (III), Th (IV), and UO2 (VI) with 5, 7-Dihydroxy-6-formyl-2-methylbenzopyran-4-one Schiff bases. Monatshefte für Chemie/Chemical Monthly 1998;129:985-98.

[19] Atta AM, Shaker N, Maysour N. Influence of the molecular structure on the chemical resistivity and thermal stability of cured Schiff base epoxy resins. Progress in organic coatings 2006;56:100-10.

[20] Jia J-H, Tao X-M, Li Y-J, Sheng W-J, Han L, Gao J-R, et al. Synthesis and third-order optical nonlinearities of ferrocenyl Schiff base. Chemical Physics Letters 2011;514:114-8.

[21] Rosu T, Pasculescu S, Lazar V, Chifiriuc C, Cernat R. Copper (II) complexes with ligands derived from 4-amino-2, 3-dimethyl-1-phenyl-3-pyrazolin-5-one: synthesis and biological activity. Molecules 2006;11:904-14.

[22] Gwaram NS, Ali HM, Khaledi H, Abdulla MA, Hadi AHA, Lin TK, et al. Antibacterial evaluation of some Schiff bases derived from 2-acetylpyridine and their metal complexes. Molecules 2012;17:5952-71.

[23] Joshi K, Pancholi A, Pandya K, Thakar A. Synthesis, characterization and antibacterial activity of novel Schiff base derived from 4-acetyl-3-methyl-1-(4'-Methyl-Phenyl)-2-Pyrazolin-5-one and its transition metal complexes. International Journal of Research in Chemistry and Environment 2011;1:263-9.

[24] Mishra AP, Mishra R, Jain R, Gupta S. Synthesis of New VO (II), Co (II), Ni (II) and Cu (II) Complexes with Isatin-3-Chloro-4-Floroaniline and 2-Pyridinecarboxylidene-4-Aminoantipyrine and their Antimicrobial Studies. Mycobiology 2012;40:20-6.

[25] Omar M, Mohamed G, Hindy A. Transition metal complexes of heterocyclic Schiff base. Journal of thermal analysis and calorimetry 2006;86:315-25.

[26] Pouralimardan O, Chamayou A-C, Janiak C, Hosseini-Monfared H. Hydrazone Schiff base-manganese (II) complexes: Synthesis, crystal structure and catalytic reactivity. Inorganica chimica acta 2007;360:1599-608.

[27] Krishnapriya K, Kandaswamy M. Coordination properties of a dicompartmental ligand with tetra-and hexadentate coordination sites towards copper (II) and nickel (II) ions. Polyhedron 2005;24:113-20.

[28] MOHAMED GG, Omar MM, Hindy AM. Metal complexes of Schiff bases: preparation, characterization, and biological activity. Turkish Journal of Chemistry 2006;30:361-82.

[29] Canpolat E, Kaya M. Studies on mononuclear chelates derived from substituted Schiff Base ligands: Synthesis and characterization of a new 5-methoxysalicyliden-p-aminoacetophenoneoxime and its complexes with Co (II), Ni (II), Cu (II), and Zn (II). Russian Journal of Coordination Chemistry 2005;31:790-4.

[30] Barwiolek M, Szlyk E, Surdykowski A, Wojtczak A. New nickel (ii) and copper (ii) complexes with unsymmetrical Schiff bases derived from (1 R, 2 R)(−) cyclohexanediamine and the application of Cu (ii) complexes for hybrid thin layers deposition. Dalton Transactions 2013;42:11476-87.

[31] Fernandez G. JM; del Rio-Portilla, F.; Quiroz-Garcia, B.; Toscano, RA; Salcedo, R. J Mol Struct 2001;561:197.

[32] Tümer M, Akgün E, Toroğlu S, Kayraldiz A, Dönbak L. Synthesis and characterization of Schiff base metal complexes: their antimicrobial, genotoxicity and electrochemical properties. Journal of Coordination Chemistry 2008;61:2935-49.

[33] Aranha PE, dos Santos MP, Romera S, Dockal ER. Synthesis, characterization, and spectroscopic studies of tetradentate Schiff base chromium (III) complexes. Polyhedron 2007;26:1373-82.

[34] Champouret YD, Fawcett J, Nodes WJ, Singh K, Solan GA. Spacially confined M2 centers (M= Fe, Co, Ni, Zn) on a sterically bulky binucleating support: Synthesis, structures and ethylene oligomerization studies. Inorganic chemistry 2006;45:9890-900.

[35] Biswas C, Drew MG, Figuerola A, Gómez-Coca S, Ruiz E, Tangoulis V, et al. Magnetic coupling in trinuclear partial cubane copper (II) complexes with a hydroxo bridging core and peripheral phenoxo bridges from NNO donor Schiff base ligands. Inorganica Chimica Acta 2010;363:846-54.

[36] Pucci D, Bellusci A, Crispini A, Ghedini M, La Deda M. Synthesis and aggregation phenomena of multifunctional Schiff bases and Ni (II) complexes: an X-ray investigation. Inorganica chimica acta 2004;357:495-504.

[37] Brodowska K, Łodyga-Chruścińska E. Schiff bases–interesting range of applications in various fields of science. CHEMIK nauka-technika-rynek 2014;1:129-34.

[38] Rodríguez-Argüelles MC, López-Silva EC, Sanmartín J, Pelagatti P, Zani F. Copper complexes of imidazole-2-, pyrrole-2-and indol-3-carbaldehyde thiosemicarbazones: inhibitory activity against fungi and bacteria. Journal of inorganic biochemistry 2005;99:2231-9.

[39] Prakash A, Adhikari D. Application of Schiff bases and their metal complexes-A Review. Int J Chem Tech Res 2011;3:1891-6.

[40] Hamada Y, Sano T, Fujita M, Fujii T, Nishio Y, Shibata K. Blue electroluminescence in thin films of azomethin-zinc complexes. Japanese Journal of Applied Physics 1993;32:L511.

[41] Hamada Y, Sano T, Fujii H, Nishio Y, Takahashi H, Shibata K. White-light-emitting material for organic electroluminescent devices. Japanese journal of applied physics 1996;35:L1339.

[42] Kawamoto T, Nishiwaki M, Tsunekawa Y, Nozaki K, Konno T. Synthesis and characterization of luminescent zinc (II) and cadmium (II) complexes with N, S-chelating Schiff base ligands. Inorganic chemistry 2008;47:3095-104.

[43] Wang PH, Keck JG, Lien EJ, Lai MM. Design, synthesis, testing, and quantitative structure-activity relationship analysis of substituted salicylaldehyde Schiff bases of 1-amino-3-hydroxyguanidine tosylate as new antiviral agents against coronavirus. Journal of medicinal chemistry 1990;33:608-14.

[44] Qureshi MS, bin Mohd Yusoff AR, Shah A, Nafady A. A new sensitive electrochemical method for the determination of vanadium (IV) and vanadium (V) in Benfield sample. Talanta 2015;132:541-7.

[45] Huang Y, Liu B, Yu Z, Zi Y. Luminescence quenching effect for the interaction of prulifloxacin with trypsin–Britton–Robinson buffer solution system. Journal of Luminescence 2010;130:360-4.

[46] Dolomanov OV, Bourhis LJ, Gildea RJ, Howard JA, Puschmann H. OLEX2: a complete structure solution, refinement and analysis program. Journal of Applied Crystallography 2009;42:339-41.

[47] Rauf A, Shah A, Abbas S, Rana UA, Khan SU-D, Ali S, et al. Synthesis, spectroscopic characterization and pH dependent photometric and electrochemical fate of Schiff bases. Spectrochimica Acta Part A: Molecular and Biomolecular Spectroscopy 2015;138:58-66.

[48] Eloff J. A sensitive and quick microplate method to determine the minimal inhibitory concentration of plant extracts for bacteria. Planta medica 1998;64:711-3.

[49] Eloff J. The antibacterial activity of 27 southern African members of the Combretaceae. South African Journal of Science 1999;95:148-52.

[50] Skehan P, Storeng R, Scudiero D, Monks A, McMahon J, Vistica D, et al. New colorimetric cytotoxicity assay for anticancer-drug screening. Journal of the National Cancer Institute 1990;82:1107-12.

[51] Rauf A, Shah A, Khan AA, Shah AH, Abbasi R, Qureshi IZ, et al. Synthesis, pH dependent photometric and electrochemical investigation, redox mechanism and biological applications of novel Schiff base and its metallic derivatives. Spectrochimica Acta Part A: Molecular and Biomolecular Spectroscopy 2017.

[52] Shuja S, Ali S, Shahzadi S, Labat G, Stoeckli-Evans H. 3-(4-Bromophenyliminomethyl) benzene-1, 2-diol. Acta Crystallographica Section E: Structure Reports Online 2006;62:o4789-o90.

[53] Khalil MM, Ismail EH, Mohamed GG, Zayed EM, Badr A. Synthesis and characterization of a novel schiff base metal complexes and their application in determination of iron in different types of natural water. Open Journal of Inorganic Chemistry 2012;2:13.

[54] Reddy SL, Reddy GS, Endo T. Electronic (absorption) spectra of 3d transition metal complexes: INTECH Open Access Publisher; 2012.

[55] Munir S, Shah A, Rauf A, Badshah A, Lunsford SK, Hussain H, et al. Redox behavior of a novel menadiol derivative at glassy carbon electrode. Electrochimica Acta 2013;88:858-64.

[56] Herries D. Alkaline phosphatase: By RB McComb, GN Bowers, Jr and S Posen. pp 986. Plenum Press, New York and London. 1979. $75 ISBN 0□306□40214□9. Biochemical Education 1981;9:76-.

[57] Shephard M, Peake M. Quantitative method for determining serum alkaline phosphatase isoenzyme activity I. Guanidine hydrochloride: new reagent for selectively inhibiting major serum isoenzymes of alkaline phosphatase. Journal of clinical pathology 1986;39:1025-30.

[58] Lorente JA, Valenzuela H, Morote J, Gelabert A. Serum bone alkaline phosphatase levels enhance the clinical utility of prostate specific antigen in the staging of newly diagnosed prostate cancer patients. European journal of nuclear medicine 1999;26:625-32.

[59] Urquiza NM, Islas MS, Dittler ML, Moyano MA, Manca SG, Lezama L, et al. Inhibition behavior on alkaline phosphatase activity, antibacterial and antioxidant activities of ternary methimazole–phenanthroline–copper (II) complex. Inorganica Chimica Acta 2013;405:243-51.

[60] Tankeo SB, Damen F, Sandjo LP, Celik I, Tane P, Kuete V. Antibacterial activities of the methanol extracts, fractions and compounds from Harungana madagascariensis Lam. ex Poir.(Hypericaceae). Journal of ethnopharmacology 2016;190:100-5.

[61] Prajitha V, Thoppil J. Cytotoxic and apoptotic activities of extract of Amaranthusspinosus L. in Allium cepa and human erythrocytes. Cytotechnology 2016:1-11.

[62] Alam AK, Hossain AS, Khan MA, Kabir SR, Reza MA, Rahman MM, et al. The Antioxidative Fraction of White Mulberry Induces Apoptosis through Regulation of p53 and NFκB in EAC Cells. PloS one 2016;11:e0167536.

Table 1. Thermogravimetric Analysis data of metal (II) complexes

Complexes	Temp. range ^{o}C	Evolved components	% Weight loss		% Residue	
			Observed	Calculated	Observed	Calculated
ZnL_2^1	320-358	$C_{26}H_{18}Cl_2N_2O_2$	82.78	88.57	ZnO_2 17.22	17.43
ZnL_2^2	375-420	$C_{26}H_{18}Br_2N_2O_2$	84.20	84.96	ZnO_2 16.80	15.03
CoL_2^1	540-580	$C_{26}H_{18}$ $Cl_2N_2O_3$	86.92	86.43	CoO 13.08	13.56
CoL_2^2	380-431	$C_{26}H_{18}$ $Cl_2N_2O_3$	88.92	88.31	CoO 11.08	11.68

Table 2. Crystal data and structure refinement for ***HL*[1]**

Identification code	***HL*[1]**
Empirical formula	$C_{13}H_{10}NO_2Cl$
Formula weight	247.67
Temperature/K	100
Crystal system	triclinic
Space group	P-1
a/Å	6.0176(6)
b/Å	8.7051(8)
c/Å	11.6778(11)
α/°	85.304(4)
β/°	80.991(4)
γ/°	70.664(4)
Volume/Å^3	569.81(10)
Z	2
ρ_{calc}mg/mm^3	1.444
m/mm^{-1}	2.877
F(000)	256.0
Crystal size/mm^3	0.25 × 0.2 × 0.04
2Θ range for data collection	7.668 to 140.152°
Index ranges	$-7 \le h \le 7$, $-10 \le k \le 10$, $-14 \le l \le 14$
Reflections collected	19056
Independent reflections	2134[R(int) = 0.0471]
Data/restraints/parameters	2134/0/163
Goodness-of-fit on F^2	1.058
Final R indexes [I>=2σ (I)]	R_1 = 0.0367, wR_2 = 0.1008
Final R indexes [all data]	R_1 = 0.0370, wR_2 = 0.1012
Largest diff. peak/hole / e Å^{-3}	0.24/-0.31

Table 3 Selected experimental and calculated geometric parameters for ***HL*[1]**

			***HL*[1]** (exp)	***HL*[1]** (calc)	Δ
Bond Distance (A˚)					
Cl1	C11		1.743(15)	1.757	0.014
O1	C2		1.359(17)	1.351	-0.008
O2	C3		1.369(18)	1.361	-0.008
N1	C7		1.287(19)	1.289	0.002
N1	C8		1.416(19)	1.407	-0.009
C1	C7		1.448(2)	1.449	0.001
Bond Angles (˚)					
C7	N1	C8	119.69(12)	121.25	1.56
C2	C1	C7	120.54(13)	120.56	0.02
C6	C1	C2	119.05(14)	119.02	-0.03
O1	C2	C1	121.87(13)	123.39	1.52
O2	C3	C4	118.74(13)	120.32	1.58
N1	C7	C1	121.58(13)	122.26	0.68
C9	C8	C13	119.46(14)	118.84	-0.62
C13	C8	N1	118.49(13)	118.04	-0.45
C10	C11	Cl1	119.10(12)	119.52	0.42

Table 4. Hydrogen-bonding geometry (A, °) for ***HL*[1]**

D	H	A	d(D-H)/Å	d(H-A)/Å	d(D-A)/Å	D-H-A/°
O1	H1	N1	0.92(2)	1.73(2)	2.5761(16)	152(2)
O2	H2	O1	0.80(3)	2.08(3)	2.7789(15)	146(2)

Table 5. Selected photometric parameters of ligands and metal complexes

Compounds	λ_{max} (nm)	ε ($M^{-1}cm^{-1}$) × 10^{-4}	pK_a
HL^1	222	3.42	7.0
HL^2	226	2.03	6.0
ZnL_2^1	219	5.61	-
ZnL_2^2	232	4.32	-
CoL_2^1	241	5.58	-
CoL_2^2	245	6.07	-

Table 6. Selected computational parameters of ligands and metal complexes calculated by RB3LYP set using DFT method in GAUSSIAN 09 software

	HL^1	HL^2	ZnL_2^1	ZnL_2^2	CoL_2^1	CoL_2^2
Charge	0	0	0	0	0	0
Spin	Singlet	Singlet	Singlet	Singlet	Doublet	Doublet
Dipole Moment (D)	4.400	4.815	6.140	6.543	6.233	6.660
Total Energy (kev)	-31.581	-88.829	-111.319	-225.815	-100.579	-215.075
E_{HOMO} (ev)	-0.207	-0.205	-0.217	-0.214	-0.216	-0.212
E_{LUMO} (ev)	-0.089	-0.086	-0.088	-0.085	-0.094	-0.086
ΔE gap (ev)	0.118	0.119	0.129	0.129	0.122	0.126
Ionization Energy ($kJmol^{-1}$)	19.972	19.779	20.937	20.648	20.841	20.455
Electron Affinity ($kJmol^{-1}$)	8.587	8.298	8.491	8.201	9.070	8.298
Electronegativity ($kJmol^{-1}$)	-0.148	-0.146	-0.152	-0.150	-0.155	-0.149
Point Group	C1	C1	C1	C1	C1	C1

Table 7. MIC of Schiff bases and metal complexes against *E. coli* and *S. aureus* bacteria

Compounds	***E. coli* (µg/ml)**	***S. aureus* (µg/ml)**
HL^1	16	32
ZnL_2^1	64	>128
CoL_2^1	128	128
HL^2	64	64
ZnL_2^2	>128	>128
CoL_2^2	>128	>128
Standard Control (Ceftriaxone)	0.5	0.25

DMSO concentration was less than 2.5%. The activity of compounds is significant when MIC<10 mg/mL, moderate when 10<MIC<100 mg/mL and low when MIC>100 mg/mL [60].

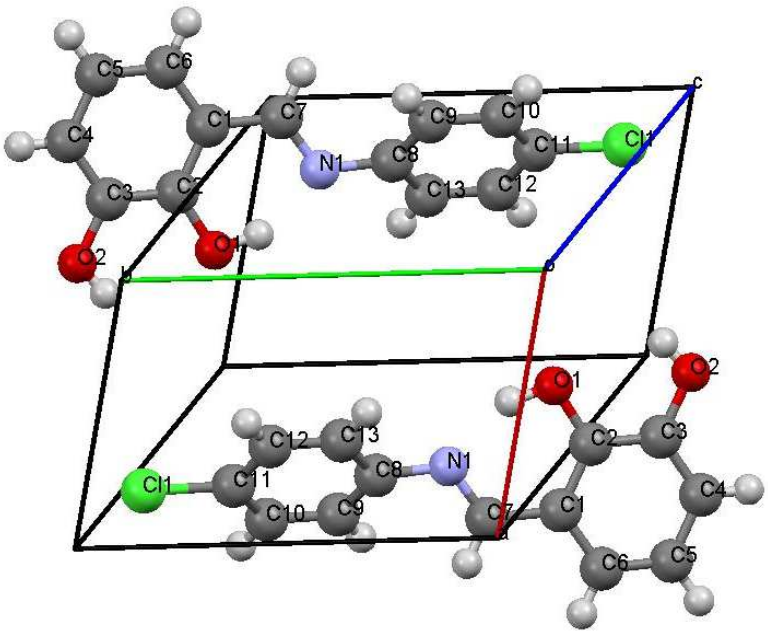

Fig. 1. Crystal packing of HL^1 along with numbering scheme and unit cell dimensions

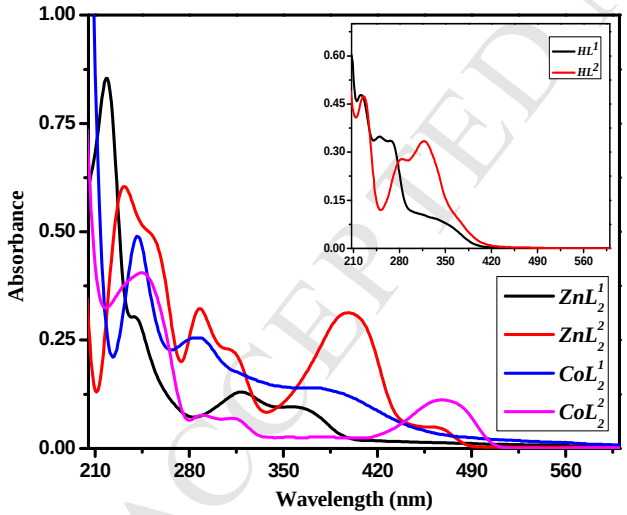

Fig. 2. UV-Visible spectra of 13.8 µM HL^1, HL^2, ZnL_2^1, CoL_2^1, ZnL_2^2 and CoL_2^2

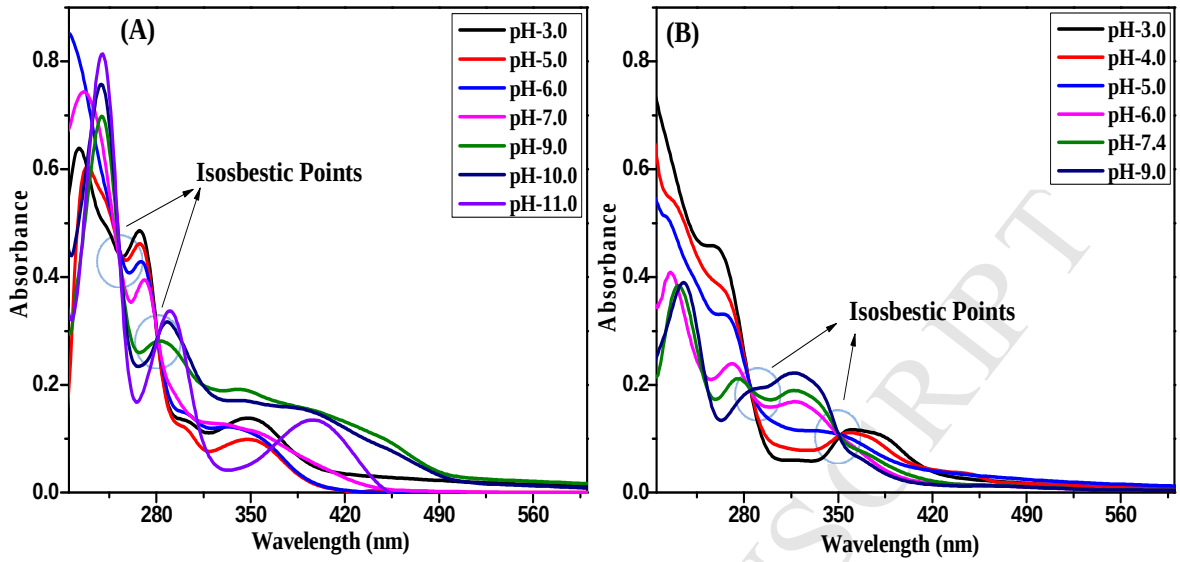

Fig. 3. UV-Vis spectra of 20 μM $\boldsymbol{HL^1}$ (A) and $\boldsymbol{HL^2}$ (B) in different pH media

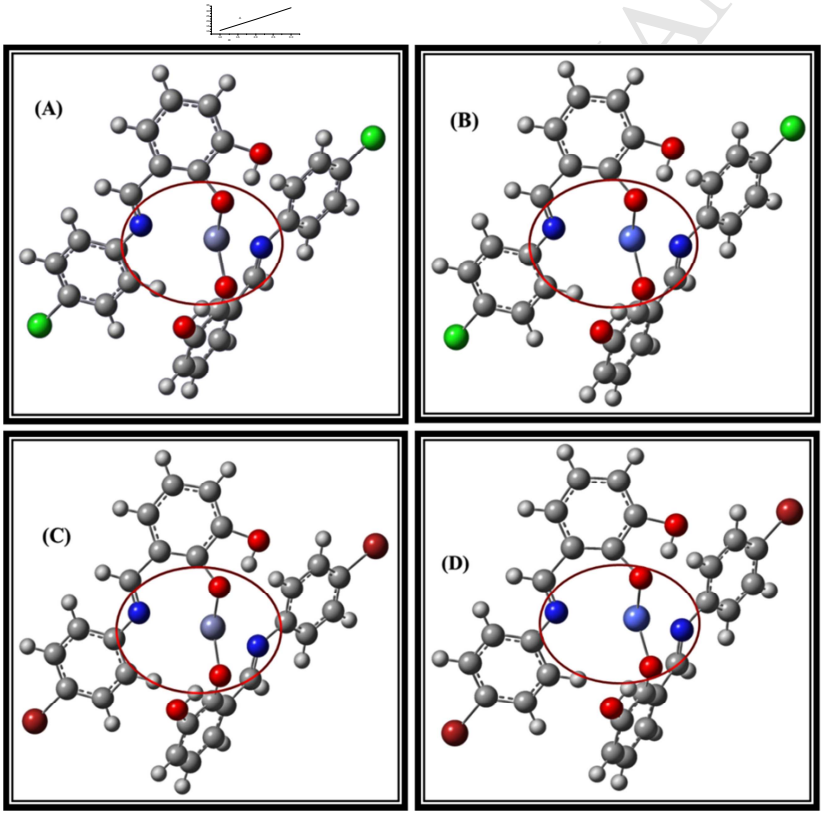

Fig. 4. Geometries of metal complexes (A) $\boldsymbol{ZnL_2^1}$ (B) $\boldsymbol{CoL_2^1}$ (C) $\boldsymbol{ZnL_2^2}$ (D) $\boldsymbol{CoL_2^2}$ optimized using DFT calculation

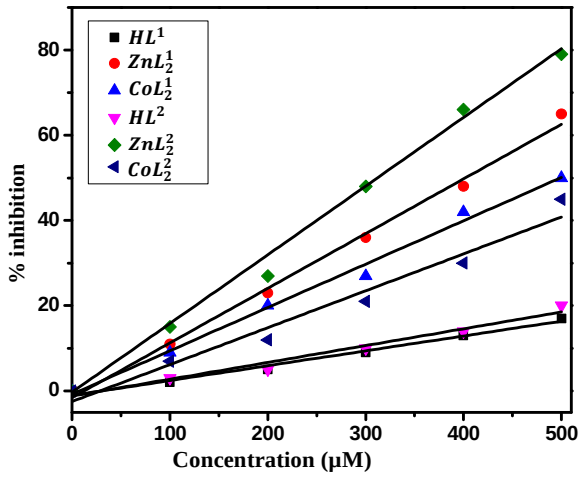

Fig. 5. Inhibition profile of alkaline phosphatase at different concentrations of ligands and their complexes

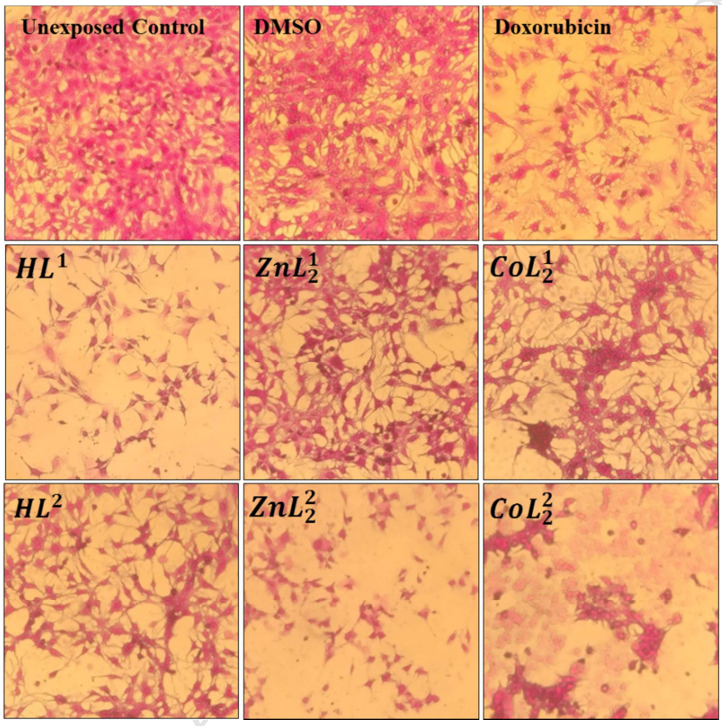

Fig. 6. Morphological effects of the synthesized Schiff bases and their metal complexes ($\boldsymbol{HL^1}$, $\boldsymbol{HL^2}$, $\boldsymbol{ZnL_2^1}$, $\boldsymbol{ZnL_2^2}$, $\boldsymbol{CoL_2^1}$ and $\boldsymbol{CoL_2^2}$) on HepG2 cells. Unexposed, DMSO (negative control) and Doxorubicin (positive control) were included as experimental controls.

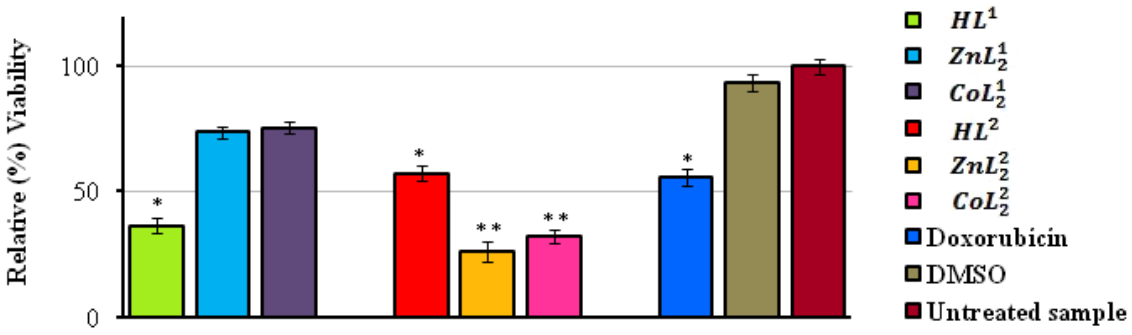

Fig. 7. Effect of the synthesized Schiff bases and their metal complexes ($\boldsymbol{HL^1}$, $\boldsymbol{HL^2}$, $\boldsymbol{ZnL_2^1}$, $\boldsymbol{ZnL_2^2}$, $\boldsymbol{CoL_2^1}$ and $\boldsymbol{CoL_2^2}$) on the viability of HepG2 cells. Exponentially growing cultures were treated with the compounds (200 µg/ml) for 24 h and percentage viabilities (mean ± std.dev) were calculated relative to the unexposed samples using SRB assay. *P < 0.01 when compared to untreated control sample, **P < 0.01 in comparison with respective Schiff base (two tailed t-test).

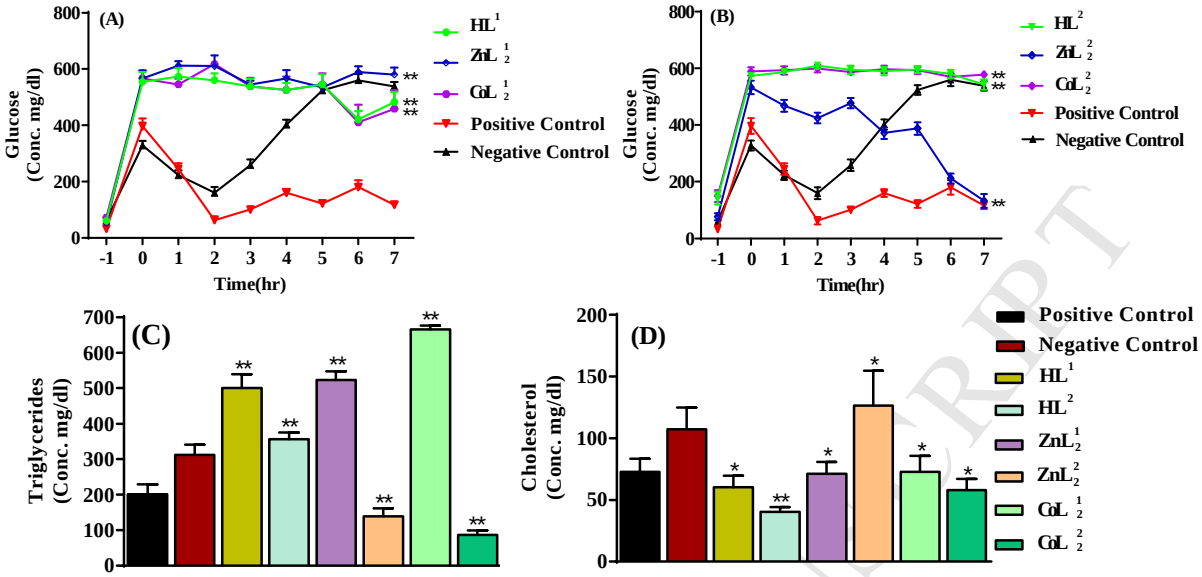

Fig. 8. Glucose (A & B), triglycerides (C) and cholesterol (D) concentrations following treatment with synthesized Schiff bases and their metal complexes ($\boldsymbol{HL^1}$, $\boldsymbol{HL^2}$, $\boldsymbol{ZnL_2^1}$, $\boldsymbol{ZnL_2^2}$, $\boldsymbol{CoL_2^1}$ and $\boldsymbol{CoL_2^2}$); control groups were treated with glibenclamide, an antidiabetic drug, whereas negative control was treated with alloxan monohydrate. Note that the complex $\boldsymbol{ZnL_2^2}$has shown significant antidiabetic character with decrease in the triglyceride concentration while elevated the serum cholesterol level drastically. Results for other compounds are also represented. **P < 0.001 and *P < 0.05.

Highlights

- Two Schiff bases and their four complexes were successfully synthesized and characterized
- Detailed photometric response was evaluated in a wide pH range
- Experimental results were found in good agreement with the computational results
- The synthesized compounds were screened for various biological activities